Wake potential in the vicinity of a surface

F. J. García de Abajo and P. M. Echenique

Departmento de Física de Materiales, Facultad de Química, Universidad del País Vasco, Apartado 1072,
20080 San Sebastián, Spain

The wake potential associated with the passage of a swift charged particle through matter in the vicinity of a solid-vacuum surface is studied. Full results of the wake potential as a function of space and time when the particle moves parallel with and perpendicular to the surface are presented. Two different approaches are followed: a dielectric analysis based upon the specular-reflection model and a Hamiltonian treatment of the problem. Several different dielectric functions are used to describe the bulk solid. Nonlocal dispersion effects are investigated. The influence of damping on the induced potential and its velocity dependence are studied.

I. INTRODUCTION

A charged particle moving near a material medium modifies the distribution of charges in that medium. Knowledge of the resulting potential allows us to study problems of binding and scattering of that particle.

The purpose of the present work is to study the real potential distribution originated by a swift charged particle that moves with constant velocity in the vicinity of a plane solid-vacuum surface. This matter has received much attention in the past mainly related to the value of the induced potential at the position of the particle itself. Ritchie[1] studied the excitation of surface plasmons by electrons. Takimoto[2] studied dynamical corrections to the classical image potential in the case of thin films. Surface excitations were shown to be important in the van der Waals force between two surfaces[3] and in the interaction of a charge with a surface.[4-8] Dynamical corrections to the image potential were achieved with[8-10] and without[11-13] inclusion of spatial dispersion in the response function. It was found that dispersion becomes important at small distances from the surface, where the particle may couple to short-wavelength modes of the solid. More sophisticated models have also been employed. Flores and García-Moliner[14] gave a full quantum-mechanical solution to the self-energy[15] of a nonrecoiled particle moving near a surface. Echenique et al.[16] followed a Hamiltonian approach[4,5] and included dispersion through a surface-plasmon dispersion relation proposed by them. Sols and Ritchie[17] have presented an extensive study of the self-energy of a light particle, which includes recoil, for motion inside and outside a solid following the method established by Manson and Ritchie.[18] This method has been extended by Zheng, Ritchie, and Manson[19] to include high-order corrections to the image potential. Eriksson, Karlsson, and Wijewardena[20] have evaluated the potential at the surface in the hydrodynamic approximation thanks to a generalization of the method employed by Heinrichs,[9] equivalent to the specular-reflection model that is discussed below.[21,22]

Here we are concerned with the study of the scalar potential engendered by a swift particle moving near a sur-

face. By analogy to the bulk wave potential,[23-25] we denote it surface wake potential. Knowledge of the spatial and time dependence of the surface wake is essential when dealing with electron production by swift ions incident on solids and in the transport of those electrons. This is the case in convoy-electron emission,[26] in grazing-incidence electron-production experiments,[27] in the generation of shock electrons,[28] in secondary electron emission,[29] and in the phenomenon of wake-riding electrons.[24] The latter have been the subject of recent experimental[30] and theoretical[31] work. Iitaka et al.[32] have recently explained the acceleration effect measured by Koyama et al.[33] on convoy electrons produced in grazing incidence of heavy ions on a metal surface in terms of the interaction of those electrons with the surface wake set up by the ions. Specular reflection of ions at a surface is also affected by the induced potential.[34] The surface wake plays an important role in the dynamics of neighboring ions moving near a surface[35] and in the Coulomb explosion of molecular ions induced by surface interaction.[36]

The organization of this paper is as follows: Section II approaches the problem for a nondispersive medium. In Sec. III the basic equations for the potential in the dielectric formalism are derived, making use of the specular-reflection model. Several models for the bulk dielectric functions are considered. In Sec. IV we summarize the results obtained from a Hamiltonian formulation of the problem. In Secs. V and VI the main numerical results for the cases of parallel and perpendicular motion are discussed together with the corrections to the classical image potential. The main conclusions are offered in Sec. VII. Atomic units will be used throughout this paper unless otherwise specified.

II. LOCAL RESPONSE FUNCTION

Many properties of the interface between two media can be analyzed by considering that they are undispersive,[37] in that the appropriate dielectric response functions may be considered to depend only on frequency. Then, the scalar potential can be simply derived by solv-

ing the Poisson equation,[13,38] taking the dielectric function as $\epsilon(\mathbf{r},\omega) = \epsilon(\omega)\Theta(-z) + \Theta(z)$, where $\Theta(z)$ is the Heaviside step function, and applying suitable matching conditions or, equivalently, by using the method of images.

The problem we are dealing with concerns a swift charged point particle with charge Z_1, which is traveling with velocity $\mathbf{v}$ in the vicinity of a planar solid-vacuum surface. The notation $\mathbf{r} = (\mathbf{R},z)$, $\mathbf{k} = (\mathbf{Q},k_z)$, and $\mathbf{v} = (\mathbf{V}_\parallel, v_z)$ will be used hereafter. $\mathbf{R}$, $\mathbf{Q}$, and $\mathbf{V}_\parallel$ represent components parallel with the surface. The z axis is

chosen in the perpendicular direction. The solid is considered to be contained in the region $z < 0$. The trajectory of the particle, whose recoil is assumed to be negligible, is described by the equation $\mathbf{r} = \mathbf{v}t$. The integration of the Poisson equation is done more easily in the Fourier-transform space. The homogeneous solutions in the bulk and in the vacuum introduce two constants of integration that are determined by the matching conditions, which are the continuity of the potential and the electric displacement. Finally, the induced potential reads

$$\phi^{\text{ind}}(\mathbf{r},t) = \phi(\mathbf{r},t) - \frac{Z_1}{|\mathbf{r}-\mathbf{v}t|}$$

$$= \frac{Z_1}{2\pi^2 |v_z|} \int d\mathbf{Q} \int d\omega \frac{e^{i(\mathbf{Q}\cdot\mathbf{R}-\omega t)}}{\tilde{k}^2} \left\{ \left[\frac{1-\epsilon(\omega)}{1+\epsilon(\omega)} \right] e^{-Q|z|} \left[\Theta(z) - \frac{\Theta(-z)}{\epsilon(\omega)} \right] + e^{i\tilde{\omega}z/v_z} \left[\frac{1}{\epsilon(\omega)} - 1 \right] \Theta(-z) \right\} , \quad (2.1)$$

where $\tilde{\omega} = \omega - \mathbf{Q}\cdot\mathbf{V}_\parallel$ and $\tilde{k}^2 = Q^2 + \tilde{\omega}^2/v_z^2$. The second term inside the curly brackets in this expression leads to the oscillatory bulk wake potential[23–25] generated by the charged particle when it moves deep inside the bulk material.

The case of motion parallel with the surface consists in taking the limit $v_z \to 0$ in Eq. (2.1) while keeping $v_z t = z_0$ constant, where z_0 is the z coordinate of the particle. In this case the surface wake potential for an external trajectory $(z_0 > 0)$ is symmetric with respect to the surface:

$$\phi_\parallel^{\text{ind}}(\mathbf{r},t) = \frac{Z_1}{2\pi} \int \frac{d\mathbf{Q}}{Q} e^{i\mathbf{Q}\cdot\tilde{\mathbf{R}}} e^{-Q(|z_0|+|z|)} \frac{1-\epsilon(\omega)}{1+\epsilon(\omega)} , \quad (2.2)$$

where $\tilde{\mathbf{R}} = \mathbf{R} - \mathbf{V}_\parallel t$ and $\omega = \mathbf{Q}\cdot\mathbf{V}_\parallel$. For an inner trajectory $(z_0 < 0)$ one obtains

$$\phi_\parallel^{\text{ind}}(\mathbf{r},t) = \frac{Z_1}{2\pi} \int \frac{d\mathbf{Q}}{Q} e^{i\mathbf{Q}\cdot\tilde{\mathbf{R}}} \left[e^{-Q(|z_0|+|z|)} \frac{1-\epsilon(\omega)}{1+\epsilon(\omega)} \left\{ \Theta(z) - \frac{\Theta(-z)}{\epsilon(\omega)} \right\} + e^{-Q|z-z_0|} \left\{ \frac{1}{\epsilon(\omega)} - 1 \right\} \Theta(-z) \right] , \quad (2.3)$$

where the second set of curly braces represents again the bulk wake potential.

Expressions (2.1)–(2.3) can be used with any frequency-dependent dielectric function. In a simple metal $\epsilon(\omega)$ is given by the classical approximation

$$\epsilon(\omega) = 1 - \frac{\omega_p^2}{\omega(\omega+i\gamma)} , \quad (2.4)$$

where $\omega_p = (4\pi n)^{1/2}$ is the classical plasma frequency of a free-electron gas with density n and γ is an infinitesimal positive quantity representing the damping of the plasma mode. Choosing $\mathbf{V}_\parallel = (v,0)$ parallel with the x direction, taking the z inverse Fourier transform in Eqs. (2.2) and (2.3), and performing the Q_x integration, the induced potential can be put in the form

$$\phi_\parallel^{\text{ind}}(\mathbf{r},t) = -\frac{\omega_s Z_1}{v} \int_0^\infty dq\, J_0 \left[q\frac{L\omega_s}{v} \right] \frac{e^{-q|\tilde{x}|\omega_s/v}}{1+q^2} + \frac{2\omega_s Z_1}{v}\Theta(-\tilde{x})\sin\frac{\omega_s\tilde{x}}{v} K_0 \left[\frac{L\omega_s}{v} \right]$$

$$+ \left\{ -\frac{\omega_p Z_1}{v} \int_0^\infty dq \left[J_0 \left[q\frac{N\omega_p}{v} \right] - J_0 \left[q\frac{L\omega_p}{v} \right] \right] \frac{e^{-q|\tilde{x}|\omega_p/v}}{1+q^2} \right.$$

$$\left. + \frac{2\omega_p Z_1}{v}\Theta(-\tilde{x})\sin\frac{\omega_p\tilde{x}}{v} \left[K_0 \left[\frac{N\omega_p}{v} \right] - K_0 \left[\frac{L\omega_p}{v} \right] \right] \right\} \Theta(-z)\Theta(-z_0) , \quad (2.5)$$

where $\omega_s = \omega_p/\sqrt{2}$ is the classical surface plasma frequency, $\tilde{x} = x - vt$, $L = \sqrt{y^2 + (|z| + |z_0|)^2}$, $N = \sqrt{y^2 + (z - z_0)^2}$, and J_0 is the Bessel function of order 0. An oscillatory contribution, whose wavelength is $2\pi v/\omega_s$, appears in the potential behind the particle and it decreases almost exponentially with L. The terms of Eq. (2.5) which contain N represent the bulk wake potential. The rest of the terms inside the set of curly braces correspond to the bulk wake potential that a particle with

opposite charge, and following a trajectory given by $\mathbf{R} = \mathbf{V}_\parallel t$ and $z = -z_0$, would create at the position $\mathbf{r}$. The integrals in (2.5) have a nonoscillatory nature (Coulomb terms[23,24]). By derivation of Eq. (2.5) one obtains the force acting on a test charge that can be further simplified when $\tilde{\mathbf{R}} = 0$.[39,40] The asymptotic behavior of Eq. (2.5) evaluated at the position of the charge provides a first correction to the classical induced potential, $-Z_1/(2|z|)$. Further, when the particle travels at the

surface, the induced potential remains finite.

If the charged particle moves in a perpendicular direction with respect to the surface ($V_\parallel = 0$, $v_z = v$) the incoming (outgoing) trajectory corresponds to $v < 0$ ($v > 0$) and

the particle finds itself in the vacuum for negative (positive) times. When $\epsilon(\omega)$ is given by Eq. (2.4), the surface-wake-induced potential reads

$$
\begin{aligned}
\phi_\perp^{ind}(\mathbf{r},t) = Z_1 \int_0^\infty dQ\, J_0(RQ) & \left\{ -\omega_s^2 \frac{e^{-Q(|z|+|vt|)}}{\omega_s^2 + Q^2 v^2} - 2\omega_s Q |v| \Theta(t) \frac{e^{-Q|z|}\sin\omega_s t}{\omega_s^2 + Q^2 v^2} \right. \\
& \left. + \Theta(-z) \left[2\omega_p Q |v| \Theta(t) \frac{e^{-Q|z|}\sin\omega_p t}{\omega_p^2 + Q^2 v^2} - \omega_p^2 \frac{e^{-Q|z-vt|}}{\omega_p^2 + Q^2 v^2} + \omega_p^2 \frac{e^{-Q(|z|+|vt|)}}{\omega_p^2 + Q^2 v^2} \right] \right\} \\
& + 2Z_1 \frac{\omega_p}{|v|} \Theta(t-z/v)\Theta(-z) \sin\frac{\omega_p(z-vt)}{v} K_0 \left[\frac{\omega_p R}{|v|} \right] .
\end{aligned}
\tag{2.6}
$$

The oscillatory terms in this formula come from the poles in the ω-complex plane of expressions involving the response function $\epsilon(\omega)$ in Eq. (2.1). They are accompanied by a factor $\Theta(t)$ that reflects the retarded character of the response. Thus, not until the particle has crossed the surface does the particle-surface interaction make any oscillatory contribution. For an incoming trajectory, the surface wake is symmetric with respect to the surface plane when the particle is still in the vacuum side because only the first term survives in (2.6) in that case. Equation (2.6) has also been obtained by Suzuki, Kitigawa, and Ohtsuki[41] from the self-consistent relation for the potential in terms of the random-phase approximation (RPA) susceptibility that they expanded up to the second order in $(E_\beta - E_\alpha)/(\omega + i\gamma)$, with E_β and E_α being the one-electron energies. They assumed a steplike profile for the electron gas density in the solid. The asymptotic behavior of the induced potential at the position of the particle is a well-established result.[9,11]

The local response contemplated in this section constitutes a crude approximation that gives realistic values only for fast particles and points in the vacuum far from the surface ($z \gg |v|/\omega_s$) or when dealing with phenomena involving high-energy transfers to the solid. i.e., when large values of ω account for the major contribution to the process under consideration. However, this simple theory reproduces most of the qualitative properties of the surface wake that are obtained with a more sophisticated model.

III. DIELECTRIC DESCRIPTION: BASIC EQUATIONS

A representation of the exact surface response function is not possible with present computational facilities. Thus a model is needed to deal with practical problems concerning surfaces. The well-known specular-reflection model (SRM), introduced in the study of the surface plasmon dispersion by Ritchie and Marusak[21] and independently discussed by Wagner,[22] constitutes a step beyond the local response of the previous section: Nonlocal effects are accounted for through the dielectric function of the bulk material $\epsilon(k,\omega)$. This model has been brought to bear on the many problems involving the interaction of charges with plane-bounded

solids.[9,14,20,42-44] In it electrons in the solid are considered to be specularly reflected at the surface and interference between the outgoing and the reflected components is neglected.[42,45,46]

The potential created by an external charge distribution $\rho^e(\mathbf{r},t)$ in the vicinity of a surface can be obtained in terms of the SRM through considering the symmetrized charge distribution $\rho_\pm^e(\mathbf{r},t)$, where the notation $A_-(\mathbf{R},z) = A(\mathbf{R},-|z|)$ and $A_+(\mathbf{R},z) = A(\mathbf{R},|z|)$ is adopted, and then solving the Poisson equation for: (i) a bulk medium described by $\epsilon(k,\omega)$ in the presence of the charge $\rho_-^e(\mathbf{r},t)$ plus a charge sheet $\sigma^-(\mathbf{R},t)\delta(z)$ located at the surface, and (ii) vacuum containing both the charge $\rho_+^e(\mathbf{r},t)$ and, as a consequence of the continuity of the electric displacement normal to the surface, the mentioned charge sheet with opposite sign, $-\sigma^-(\mathbf{R},t)\delta(z)$. The former provides the potential in the solid side ($z < 0$), while the latter applies to the vacuum side. The quantity σ^- is eliminated after imposing the continuity of the potential at the surface. Using the form

$$
f(\mathbf{r},t) = \frac{1}{(2\pi)^4} \int d\mathbf{k}\, d\omega\, f(\mathbf{k},\omega) e^{i(\mathbf{k}\cdot\mathbf{r} - \omega t)} ,
$$

for the Fourier transform and carrying out the calculations outlined above, one obtains the result

$$
\phi(\mathbf{r},t) = \phi_+(\mathbf{r},t)\Theta(z) + \phi_-(\mathbf{r},t)\Theta(-z) ,
\tag{3.1}
$$

and

$$
\phi_\pm(\mathbf{Q},z,\omega) = 4\pi[U_\pm(\mathbf{Q},z,\omega) \mp \rho^s(\mathbf{Q},\omega)\epsilon_\pm(Q,z,\omega)] ,
\tag{3.2}
$$

where

$$
U_+(\mathbf{Q},z,\omega) = \frac{1}{2\pi} \int \frac{dk_z}{k^2} \rho_+^e(\mathbf{k},\omega) e^{ik_z z} ,
$$

$$
U_-(\mathbf{Q},z,\omega) = \frac{1}{2\pi} \int \frac{dk_z}{k^2} \rho_-^e(\mathbf{k},\omega) \frac{e^{ik_z z}}{\epsilon(k,\omega)} ,
\tag{3.3}
$$

$$
\epsilon_+(Q,z,\omega) = \frac{Q}{\pi} \int \frac{dk_z}{k^2} e^{ik_z z} = e^{-Q|z|} ,
$$

$$
\epsilon_-(Q,z,\omega) = \frac{Q}{\pi} \int \frac{dk_z}{k^2} \frac{e^{ik_z z}}{\epsilon(k,\omega)} = \epsilon_s(Q,z,\omega) ,
\tag{3.4}
$$

and the quantity

$$\rho^s(\mathbf{Q},\omega)=\frac{U_+(\mathbf{Q},0,\omega)-U_-(\mathbf{Q},0,\omega)}{1+\epsilon_s(Q,\omega)} , \qquad (3.5)$$

where $\epsilon_s(Q,\omega)=\epsilon_s(Q,0,\omega)$ is the so-called surface dielectric function,[45] is related to the charge sheet through $\rho^s(\mathbf{Q},\omega)=\sigma^-(\mathbf{Q},\omega)/2Q$.

Let us consider a swift moving charge in the vicinity of a solid surface and let the particle charge and trajectory be described as in the previous section. The external charge density takes the form $\rho^e(\mathbf{r},t)=Z_1\delta(\mathbf{r}-\mathbf{v}t)$. The quantities $U_\pm$ are readily found to be

$$U_+(\mathbf{Q},z,\omega)=\frac{Z_1}{|v_z|}\left\{\frac{e^{i\tilde\omega|z|/v_z}}{\tilde{k}^2}+\frac{i\tilde\omega e^{-Q|z|}}{v_z\tilde{k}^2Q}\right\} , \qquad (3.6a)$$

$$U_-(\mathbf{Q},z,\omega)=\frac{Z_1}{|v_z|}\left\{\frac{e^{-i\tilde\omega|z|/v_z}}{\tilde{k}^2\epsilon(\tilde{k},\omega)}-\frac{i\tilde\omega e^{-Q|z|}}{v_z\tilde{k}^2Q\epsilon(\omega)}+\alpha(z)\right\} , \qquad (3.6b)$$

where $\epsilon(\omega)=\epsilon(0,\omega)$, $\tilde\omega=\omega-\mathbf{Q}\cdot\mathbf{V}_\parallel$, and $\tilde{k}^2=Q^2+\tilde\omega^2/v_z^2$. Provided that $\epsilon(k,\omega)$ has no branch points in the k_z-complex plane, one obtains

$$\alpha(z)=\frac{-2\tilde\omega}{v_z}\sum_{\mathrm{Im}k_0>0}\frac{e^{ik_0|z|}}{(Q^2+k_0^2)[k_0^2-(\tilde\omega/v_z)^2]}$$
$$\times\mathrm{Res}\left\{\frac{1}{\epsilon(k,\omega)}\right\}_{k_z=k_0} ,$$

where the sum is extended over the zeros of $\epsilon(k,\omega)$ in the upper-half k_z-complex plane. Also, from Eqs. (3.4),

$$\epsilon_s(Q,z,\omega)=\frac{e^{-Q|z|}}{\epsilon(\omega)}+\beta(z) , \qquad (3.7)$$

where

$$\beta(z)=2iQ\sum_{\mathrm{Im}k_0>0}\frac{e^{ik_0|z|}}{(Q^2+k_0^2)}\mathrm{Res}\left\{\frac{1}{\epsilon(k,\omega)}\right\}_{k_z=k_0} . \qquad (3.8)$$

When the poles k_0 in the previous sums have finite imaginary parts, $\alpha(z)$ and $\beta(z)$ go to zero like a decaying exponential in the $|z|\to\infty$ limit. However, k_0 may have an infinitesimal imaginary part coming, for instance, from the damping of the plasma modes that in the retarded response formalism used here enters the dielectric function through the substitution $\omega\to\omega+i\gamma$, $\gamma\to0+$. In this case $\alpha(z)$ and $\beta(z)$ behave like imaginary exponentials whose arguments vary with Q and ω. Nevertheless, these quantities oscillate very rapidly as $|z|$ becomes large, giving rise to a vanishing contribution to the potential in that limit.

The induced potential,

$$\phi^{\mathrm{ind}}(\mathbf{r},t)=\phi(\mathbf{r},t)-Z_1/|\mathbf{r}-\mathbf{v}t| ,$$

can be written from Eqs. (3.1)–(3.8), after some tedious but straightforward algebra, as

$$\phi^{\mathrm{ind}}_{z>0}(\mathbf{r},t)=\frac{Z_1}{2\pi^2}\int_0^\infty dQ\int_0^{2\pi}d\Theta\, e^{i\mathbf{Q}\cdot\mathbf{R}}\int_{-\infty}^\infty d\omega\, e^{-i\omega t}e^{-Q|z|}A ,$$

$$\phi^{\mathrm{ind}}_{z<0}(\mathbf{r},t)=\frac{Z_1}{2\pi^2}\int_0^\infty dQ\int_0^{2\pi}d\Theta\, e^{i\mathbf{Q}\cdot\mathbf{R}}\int_{-\infty}^\infty d\omega\, e^{-i\omega t}[B(z)-A\epsilon_s(Q,z,\omega)]+\phi^\infty(\mathbf{r}-\mathbf{v}t,\mathbf{v}) ,$$

$$(3.9)$$

where

$$A=\frac{\tilde{k}^2B(0)+(Q/|v_z|)[1/\epsilon(\tilde{k},\omega)-1]}{\tilde{k}^2[1+\epsilon_s(k,\omega)]} ,$$

$$(3.10)$$

$$B(z)=\frac{1}{|v_z|}\left[Q\alpha(z)+\frac{i\tilde\omega}{\tilde{k}^2v_z}\beta(z)\right]=-\mathrm{sgn}(v_z)\frac{2\tilde\omega Q}{\tilde{k}^2}\sum_{\mathrm{Im}k_0>0}\frac{e^{ik_0|z|}}{(k_0^2v_z^2-\tilde\omega^2)}\mathrm{Res}\left\{\frac{1}{\epsilon(k,\omega)}\right\}_{k_z=k_0} ,$$

and

$$\phi^\infty(\mathbf{r},\mathbf{v})=\frac{Z_1}{2\pi^2}\int\frac{d\mathbf{k}}{k^2}\left[\frac{1}{\epsilon(k,\mathbf{k}\cdot\mathbf{v})}-1\right]e^{i\mathbf{k}\cdot\mathbf{r}} \qquad (3.11)$$

represents the bulk wake potential in the solid[23–25] at the position $\mathbf{r}$ with respect to the particle when it moves deep inside the solid with velocity $\mathbf{v}$.

When $z\to\infty$ the contribution to ϕ^{ind} to order $1/z$ is obtained from Eqs. (3.9):

$$\phi^{\mathrm{ind}}(\mathbf{r},t)\approx\frac{1-\epsilon_0}{1+\epsilon_0}\frac{Z_1}{\sqrt{|\mathbf{R}-\mathbf{V}_\parallel t|^2+(z+v_zt)^2}} ,$$
$$z\to\infty,\ |\mathbf{r}-\mathbf{v}t|\ll z , \qquad (3.12)$$

where $\epsilon_0=\epsilon(0,0)$ is the static and local dielectric constant. This result coincides with the classical electrostatic potential. In the limit $z\to-\infty$ the induced potential reduces to the bulk wake given by Eq. (3.11).

So far no choice has been done for the bulk dielectric function, $\epsilon(k,\omega)$. It should be mentioned that when one takes a frequency-dependent response, $\alpha(z)$ and $\beta(z)$ trivially vanish and one is dealing with the undispersive case of Sec. II. Two different approximations will be considered here that go beyond the local response function.

(i) The hydrodynamic approximation (HA)[47]

$$\epsilon(k,\omega)=1+\frac{\omega_p^2}{\beta^2k^2-\omega(\omega+i\gamma)} \quad (\gamma\to0^+) , \qquad (3.13)$$

which incorporates dispersion of the plasma modes through $\beta = \sqrt{3/5}v_F$, the speed of propagation of density disturbances in an electron gas characterized by a Fermi velocity v_F. Inserting Eq. (3.13) in Eqs. (3.7) and (3.8), one obtains

$$\epsilon_s(Q,\omega) = \frac{\omega(\omega+i\gamma)e^{-Q|z|} - (Q\omega_p^2/\Lambda)e^{-\Lambda|z|}}{\omega(\omega+i\gamma) - \omega_p^2} ,$$

and from Eq. (3.10),

$$B(z) = \text{sgn}(v_z) \frac{i\widetilde{\omega}\omega_p^2 Q e^{-\Lambda|z|}}{\beta^2 \widetilde{k}^2 \Lambda\{\Lambda^2 v_z^2 + \widetilde{\omega}^2\}} ,$$

where we have made use of the fact that the only zero of

(3.13) in $\text{Im}k_z > 0$ is given by

$$\Lambda = -ik_z = \frac{1}{\beta}\sqrt{\omega_p^2 + \beta^2 Q^2 - \omega(\omega+i\gamma)} ,$$

and the square root is understood to yield $\text{Re}(\Lambda) > 0$.

(ii) The plasmon pole approximation (PLA),[48]

$$\epsilon(k,\omega) = 1 + \frac{\omega_p^2}{\omega_g^2 + \beta^2 k^2 + k^4/4 - \omega(\omega+i\gamma)} \quad (\gamma \to 0^+) ,$$

(3.14)

that retains the main features of the full RPA dielectric function. There are two poles of $\epsilon(k,\omega)$ in the upper-half k_z-complex plane: $i(Q^2 + 2\Lambda_\pm^2)^{1/2}$. Using Eq. (3.14), one obtains[16]

$$\epsilon_s(Q,z,\omega) = \frac{\omega(\omega+i\gamma)}{\Omega}e^{-Q|z|} + \frac{\omega_p^2 Q}{\Lambda_+ - \Lambda_-} \left\{ \frac{e^{-|z|(Q^2+2\Lambda_-)^{1/2}}}{\Lambda_-(Q^2+2\Lambda_-)^{1/2}} - \frac{e^{-|z|(Q^2+2\Lambda_+)^{1/2}}}{\Lambda_+(Q^2+2\Lambda_+)^{1/2}} \right\} ,$$

(3.15)

where $\Omega = \omega(\omega+i\gamma) - \Omega_0^2$, $\Lambda_\pm = \beta^2 \pm [\beta^4 + \Omega]^{1/2}$, and $\Omega_0^2 = \omega_p^2 + \omega_g^2$. The square roots in Eq. (3.15) are taken to yield a positive real part. In the same way one finds

$$B(z) = \text{sgn}(v_z) \frac{2iQ\widetilde{\omega}\omega_p^2}{\widetilde{k}^2(\Lambda_+ - \Lambda_-)} \left\{ \frac{e^{-|z|(Q^2+2\Lambda_-)^{1/2}}}{(Q^2+2\Lambda_-)^{1/2}[v_z^2(Q^2+2\Lambda_-)+\widetilde{\omega}^2]} - \frac{e^{-|z|(Q^2+2\Lambda_+)^{1/2}}}{(Q^2+2\Lambda_+)^{1/2}[v_z^2(Q^2+2\Lambda_+)+\widetilde{\omega}^2]} \right\} .$$

The asymptotic behavior of the potential must be quite similar in both the HA and the PLA cases because the only difference between these approximations is that the latter includes single-particle excitations (the term $k^4/4$) in the plasmon dispersion and this becomes important only at small distances from the surface.

Under the HA approximation the expression for the surface wake potential given by the SRM, Eqs. (3.9), coincides with the solution obtained by solving the linearized Bloch hydrodynamic equations for a jellium bounded by a rigid wall at the surface, and then imposing as matching conditions the vanishing of the normal component of the hydrodynamic velocity and the continuity of the potential and its derivative.

IV. HAMILTONIAN FORMULATION

The so-called Hamiltonian models[49−53] reduce the solid-charged particle interaction to a problem of creation and destruction of excitations in the solid with well-defined energies. They have been extensively employed in the past.[4,11,12,16−18,35,54−59] However, these do not account for the continuum of electron-hole pair excitations. Nevertheless, dispersion can be easily implemented in the plasma modes.

We restrict ourselves to the interaction of an external charged point particle with a medium via its bulk and surface plasmons. Under this assumption the Hamiltonian that describes the problem may be written as[51−53]

$$H = H_0 + H_1 ,$$

where

$$H_0 = \frac{p^2}{2M} + \sum_Q \sigma_Q a_Q^\dagger a_Q + \sum_{Q,k_z>0} \omega_k b_k^\dagger b_k$$

is the Hamiltonian of the free particle and the free medium, $a_Q^\dagger$ and $b_k^\dagger$ are the creation operators for surface and bulk plasmons, respectively, and σ_Q and ω_k are the energies of those excitations. The interaction Hamiltonian reads

$$H_1 = \int d\mathbf{r}\, \phi^s(\mathbf{r})\rho(\mathbf{r},t) ,$$

where the scalar potential operator in the Schrödinger picture,[60]

$$\phi^s(\mathbf{r}) = \sum_{Q,k_z>0} B_k b_k \sin k_z z\, e^{i\mathbf{Q}\cdot\mathbf{R}}\Theta(-z)$$

$$+ \sum_Q A_Q a_Q e^{-Q|z|} e^{i\mathbf{Q}\cdot\mathbf{R}} + \text{H.c.} ,$$

has been used, and

$$|B_k|^2 = \frac{8\pi\omega_p^2}{Vk^2\omega_k} , \quad |A_Q|^2 = \frac{\pi\omega_s^2}{SQ\sigma_Q} .$$

V is the volume of the solid and S is the area of its surface.

Let us assume that the particle has a very large mass, so that recoil is neglected. We consider a particle that moves along a straight line, so that the external charge distribution is $\rho(\mathbf{r},t) = Z_1\delta(\mathbf{r}-\mathbf{v}t)$. The notation of Sec.

II is used here. Following standard techniques,[60] the wave function in the interaction picture at the time t is readily found to be

$$|\Psi^I\rangle = \left\{ \prod_k e^{-|I_k|^2/2} e^{-iI_k^* b_k^\dagger} \right\}$$

$$\times \left\{ \prod_Q e^{-|J_Q|^2/2} e^{-iJ_Q^* a_Q^\dagger} \right\} |0\rangle ,$$

where

$$I_k = Z_1 B_k \int_{-\infty}^t dt' \sin k_z v_z t' e^{i(Q\cdot V_\parallel - \omega_k)t'} \Theta(-v_z t')$$

and

$$\phi^{\text{surf}}(r,t) = Z_1 \frac{\omega_s^2}{2\pi} \int dQ \frac{e^{-Q(|z|+|v_z t|)}}{Q} e^{iQ\cdot R} \left[\frac{\Theta(-t)}{(Q\cdot V_\parallel + iQ|v_z|)^2 - \sigma_Q^2} + \frac{\Theta(t)}{(Q\cdot V_\parallel - iQ|v_z|)^2 - \sigma_Q^2} \right]$$

$$- Z_1 \frac{\omega_s^2}{\pi} |v_z| \Theta(t) \int dQ \frac{e^{-Q|z|}}{\sigma_Q} \frac{\sin(\sigma_Q t - Q\cdot R)}{(Q\cdot V_\parallel - \sigma_Q)^2 + Q^2 v_z^2} \qquad (4.2)$$

stands for the part of the potential which originates in the interaction of the particle with the surface excitations. The bulk excitations contribute as

$$\phi^{\text{bulk}}(r,t) = [\phi^\infty(r - vt, v) - \phi^\infty(\tilde{r} - vt, v)] \Theta(-v_z t)$$

$$+ [\zeta^\infty(r, v, t) - \zeta^\infty(\tilde{r}, v, t)] \Theta(t)\text{sgn}(v_z) , \qquad (4.3)$$

where $\tilde{r} = (R, -z)$, $\phi^\infty(r, v)$ is given by Eq. (3.11) with the following dielectric function:

$$\epsilon(k, \omega) = 1 + \frac{\omega_p^2}{\omega_k^2 - \omega_p^2 - \omega(\omega + i\gamma)} , \quad \gamma \to 0^+ ,$$

similar to the PLA of Eq. (3.14), and

$$\zeta^\infty(r, v, t) = \frac{Z_1}{2\pi^2} \int \frac{dk}{k^2} \left[\frac{1}{\epsilon(k, k\cdot v)} - 1 \right] e^{ik\cdot r}$$

$$\times \left\{ \cos\omega_k t - \frac{ik\cdot v}{\omega_k} \sin\omega_k t \right\} .$$

Expression (4.3) is made up of two parts, each with different sign. They can be understood as coming from two different stimuli: one located at the position of the particle and the other at the specular image of this position with respect to the surface. Not until the particle has crossed the surface does the second bracketed term make any contribution, while the first one vanishes when the particle is outside the solid.

In computing these expressions we choose for the bulk plasmons the following dispersion relation:

$$\omega_k^2 = \omega_p^2 + \beta^2 k^2 + k^4/4 .$$

$$J_Q = Z_1 A_Q \int_{-\infty}^t dt' e^{-Q|v_z t'|} e^{i(Q\cdot V_\parallel - \sigma_Q)t'} .$$

Then the induced potential reads

$$\phi^{\text{ind}}(r,t) = \langle \Psi^I | \phi^I | \Psi^I \rangle ,$$

where

$$\phi^I = e^{iH_0 t} \phi^S e^{-iH_0 t} .$$

After very simple manipulations one finds

$$\phi(r,t) = \phi^{\text{surf}}(r,t) + \phi^{\text{bulk}}(r,t)\Theta(-z) , \qquad (4.1)$$

where

For the surface plasmon dispersion relation we adopt the one proposed in Ref. 16, in the spirit of the PLA (see Ref. 40 as well), to account for the electron-hole pair excitations in the large momentum limit:

$$\sigma_Q^2 = \omega_s^2 + \beta\omega_s Q + \eta Q^2 + Q^4/4 ,$$

where $\eta = v_F^2 - (\beta\omega_s Q_c + \omega_s^2 - Q_c^3 v_F)/Q_c^2$ and Q_c is the momentum for which the Landau cutoff intersects the surface plasmon dispersion curve: $\sigma_Q(Q_c) = Q_c[Q_c + 2v_F]/2$. The undispersive case of Sec. II is achieved through taking $\omega_k = \omega_p$ and $\sigma_Q = \omega_s$.

V. PARALLEL TRAJECTORY: $v_z = 0$

The perpendicular and parallel components of the force acting on the particle (image force) under parallel motion conditions have received great attention in the past as they could be responsible for the deflection angle in the trajectory and the energy loss suffered by the charge.[35,61,62,58] The possibility of a skipping motion of ions at the surface, where the image force plays the role of the attractive force against the planar crystal potential, has also been suggested.[63] The knowledge of the surface wake potential allows us to deal with those problems. It has been calculated by Gumbs and Glasser[44] using the SRM and the RPA dielectric function for the bulk.

The surface wake for parallel motion is obtained from the equations of the previous sections by taking the limit $v_z \to 0$ while maintaining $v_z z = z_0$ constant, where z_0 is the z coordinate of the particle that creates the wake. The results are written for $Z_1 = 1$ hereafter.

Beginning with the Hamiltonian formulation, Eq. (4.2), which gives the surface modes contribution, the potential reads as follows:

$$\phi^{\text{surf}}(r,t) = \frac{\omega_s^2}{2\pi} \int dQ \frac{e^{-Q(|z|+|z_0|)}}{Q\sigma_Q} \left\{ P\frac{\cos Q\cdot \tilde{R}}{Q\cdot V_\parallel - \sigma_Q} + \pi \sin Q\cdot \tilde{R} \, \delta(\sigma_Q - Q\cdot V_\parallel) \right\} , \qquad (5.1)$$

where $\tilde{\mathbf{R}} = \mathbf{R} - \mathbf{V}_\parallel t$.

When the particle moves in the solid side ($z_0 < 0$) the induced potential is found to be, in terms of the SRM,

$$\phi^{\mathrm{ind}}(\mathbf{r},t) = \frac{1}{2\pi}\int\frac{d\mathbf{Q}}{Q}e^{i\mathbf{Q}\cdot\tilde{\mathbf{R}}}\left\{\frac{2\epsilon_s(Q,z_0,\omega)}{1+\epsilon_s(Q,\omega)}e^{-Q|z|}\Theta(z)\right.$$

$$\left.+\left[\epsilon_s(Q,z-z_0,\omega)+\epsilon_s(Q,z+z_0,\omega)-\frac{2\epsilon_s(Q,z_0,\omega)}{1+\epsilon_s(Q,\omega)}\epsilon_s(Q,z,\omega)\right]\left[\Theta(-z)-e^{-Q|z-z_0|}\right]\right\},$$

$$(5.2)$$

where $\omega = \mathbf{Q}\cdot\mathbf{V}_\parallel$, while for a particle traveling in the vacuum ($z_0 > 0$) one gets

$$\phi^{\mathrm{ind}}(\mathbf{r},t) = \frac{1}{2\pi}\int\frac{d\mathbf{Q}}{Q}e^{i\mathbf{Q}\cdot\tilde{\mathbf{R}}}\left\{\frac{\epsilon_s(Q,\omega)-1}{\epsilon_s(Q,\omega)+1}e^{-Q|z+z_0|}\Theta(z)+\left[\frac{2e^{-Qz_0}}{\epsilon_s(Q,\omega)+1}\epsilon_s(Q,z,\omega)-e^{-Q|z-z_0|}\right]\Theta(-z)\right\}. \qquad (5.3)$$

These results reproduce previous calculations for the induced potential at the position of the particle.[43] Equation (5.1) is obtained from (5.2) and (5.3) for positive z when the surface response function is approximated by $\epsilon_s(Q,z,\omega) = \epsilon_s(Q,\omega)e^{-Q|z|}$ and

$$[\epsilon_s(Q,\omega)-1]/[\epsilon_s(Q,\omega)+1] = \omega_s^2/[\omega(\omega+i\gamma)-\sigma_Q^2],$$

$$\gamma \to 0^+.$$

The correction to the image potential $\phi^I(z)$ (defined as half the induced potential at the position of the charged particle, that creates it) with respect to the classical result, which in the case of a metal is $-1/(4z)$ [from Eq. (3.12) for $\mathbf{r} = \mathbf{v}t$ and $\epsilon_0 \to \infty$], can be derived from Eq. (5.3). Using Eqs. (3.7) and (3.8) one obtains

$$\Phi^I(z) = \frac{-1}{4z} + i\sum_{\mathrm{Im}k_0 > 0}\frac{1}{k_0^2}\mathrm{Res}\left\{\frac{1}{\epsilon(k_z,\omega)}\right\}_{k_z = k_0}\frac{1}{2z^2}$$

$$+ O\left[\frac{1}{z^3}\right].$$

When the second term in the right-hand side of this expression is evaluated utilizing the HA approximation to the dielectric function [Eq. (3.13)], it reduces to

$$\phi^I(z) = \frac{-1}{4z} + \frac{\beta}{4\omega_p}\frac{1}{z^2} + O\left[\frac{1}{z^3}\right].$$

When the PLA dielectric function is used instead one obtains

$$\phi^I(z) = \frac{-1}{4z} + \frac{[\beta^2+\sqrt{\beta^4-\Omega_0^2}]^{3/2}-[\beta^2-\sqrt{\beta^4-\Omega_0^2}]^{3/2}}{8\sqrt{2}\sqrt{\beta^4-\Omega_0^2}\,\Omega_0^3}\frac{\omega_p^2}{z^2} + O\left[\frac{1}{z^3}\right].$$

For $\beta^2 = \Omega_0$ the second term in the above expression is finite and given by $3\beta\omega_p^2/(8\sqrt{2}\Omega_0^3 z^2)$ (this happens for $r_s = 1.628$ if ω_g is 0). In the range of metallic densities and for $\omega_g = 0$ the correction introduced by the PLA to the classical image potential is between 5 and 15 % larger than the correction obtained from the HA approximation and it increases with the parameter r_s. The effect of dispersion is stronger in the PLA, but at large distances from the surface the small momentum behavior dominates in the potential, and, consequently, the electron-hole pair excitations, which the PLA incorporates through the large momentum limit in the dispersion of the bulk plasma modes, have a little effect.

The correction term in the above equations, B/z^2, is velocity independent as it comes from the small momentum limit. It can be understood as a shift in the position of the apparent image plane.[9] Thus the image potential is, to that order of approximation, that generated by a perfect metal whose apparent surface is located at $z = -4B$. Previous local density studies locate this new surface displaced toward the vacuum.[64,65] In our case it is located inside the solid because we have assumed implicitly the infinite barrier model for the surface through the

SRM. In the absence of dispersion the real surface coincides with the apparent surface. The sign of the dispersion correction to the surface plasma affects the position of the apparent surface as well.

The potential at the position of the particle has been plotted in Fig. 1 in relation to its dependence on the model (a), damping (b), and velocity (c). The SRM gives almost identical results when using both the PLA and HA approximations to the bulk dielectric function, showing that the induced potential at the position of the ion is not affected by electron-hole pair excitations. One obtains similar values for the potential when using the Hamiltonian formulation of Eqs. (4.1), (4.3), and (5.1). The induced potential reaches the bulk value ($\approx \pi\omega_p/2v$) in the solid side at a distance $|z| > \pi v/2\omega_p$ [see Fig. 1(a)]. The potential at the surface ($z = 0$) is reduced by the factor $\sqrt{2}$ with respect to the bulk value, in good agreement with the local response result. The dependence on the damping is consistent with previous calculations for the bulk wake potential:[66] the larger the damping the more attenuated the potential. Moreover, this attenuation seems to be stronger in the solid and it disappears for $z > \pi v/2\omega_s$ in the vacuum side, where the potential con-

verges to the classical limit [see Fig. 1(b)]. The induced potential seems to follow a universal curve independent of the velocity, as it may be appreciated in Fig. 1(c), in good agreement with the nonlocal description [see Eq. (2.5)].
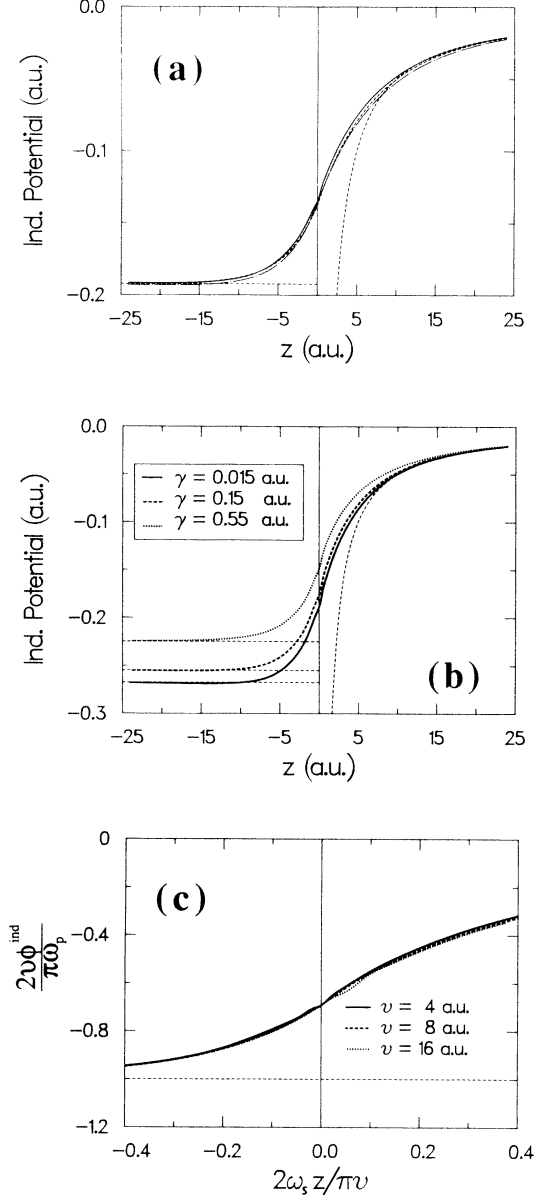

FIG. 1. Induced potential at the position of a proton moving parallel with a solid-vacuum surface as a function of the distance to the surface. The solid is in the region $z < 0$. (a) Different models have been used for the surface response with $r_s = 2$ and $\gamma = 0.015$ a.u.: local response (dashed-dotted line), SRM with the PLA dielectric function (continuous line), SRM with HA (dotted line), almost coinciding with the previous one, and Hamiltonian formulation (dashed line). The classical induced potential, $-1/2z$, and the bulk limit (quite close to $-\pi\omega_p/2v$ in all the cases) are shown as dashed lines. The velocity of the ion is $v = 5$ a.u. (b) Effect of damping using the SRM with the PLA dielectric function for $r_s = 1.6$ and damping $\gamma = 0.015, 0.15$, and 0.55 a.u. (c) Effect of the velocity using the SRM and the PLA for $r_s = 3$, $\gamma = 0.015$ a.u., and $v = 4, 8$, and 16 a.u.

In Figs. 2(a)–2(d) the surface wake potential is shown in the plane containing both the normal to the surface and the particle trajectory for different positions of the ion. It has been calculated from Eqs. (5.2) and (5.3) with the PLA approximation to the surface response given by Eq. (3.15). When the particle is moving in the vacuum side, the induced potential is almost symmetric with respect to the apparent surface plane, as in the local response approximation of Eq. (2.2). Under these circumstances a trough (a hill) is seen at a distance $\approx \pi v/2\omega_s$ ($3\pi v/2\omega_s$) behind the particle [Figs. 2(a) and 2(b)]. It has its origin in the characteristic oscillations of the surface wake potential whose wavelength is $\approx 2\pi v/\omega_s$ for an external trajectory. When the particle follows an inner trajectory, but stays close enough to the surface ($|z| < \pi v/2\omega_s$), the potential shows oscillations of frequency ω_s and ω_p [see Fig. 2(c)] as predicted by the simple model of Eq. (2.5). As the ion travels deeper inside the solid, the latter becomes dominant [Figs. 2(c) and 2(d)]. For an external trajectory the induced potential in the vacuum in a plane parallel with the surface oscillates with frequency ω_s as well and it increases when $|z| + |z_0|$ decreases [see Eq. (5.3)] as can be seen in Fig. 2(e).

VI. PERPENDICULAR TRAJECTORY: $V_\parallel = 0$

A great deal of work has been concerned with the image potential created by a charge moving in the direction perpendicular to the surface.[8–14,16,17,20] Here we picture the induced potential as a space- and time-dependent function. The problem has axial symmetry and consequently the space dependence of the potential is realized through $R = |\mathbf{R}|$ and z. The Θ integration in (3.9) and (4.2) can be performed directly, giving rise to a factor $J_0(RQ)$.

Using the Hamiltonian formulation, the potential outside the solid reads from Eq. (4.2),[16]

$$\phi^{surf}(\mathbf{r},t) = -\omega_s^2 \int_0^\infty dQ\, J_0(RQ) \frac{e^{-Q(|z|+|vt|)}}{\sigma_Q^2 + Q^2 v^2}$$
$$-2\omega_s^2 |v| \Theta(t) \int_0^\infty dQ\, J_0(RQ) \frac{Qe^{-Q|z|}}{\sigma_Q}$$
$$\times \frac{\sin\sigma_Q t}{\sigma_Q^2 + Q^2 v^2}. \quad (6.1)$$

The induced potential at the position of the particle remains finite in this approximation when it is at the surface. Ignoring the Q^4 term in σ_Q, one obtains

$$\phi^{ind}(\mathbf{r} = \mathbf{v}t = 0) = \frac{-2\omega_s}{\sqrt{4(\eta + v^2) - \beta^2}}$$
$$\times \left\{ \frac{\pi}{2} - \arctan \frac{\beta}{\sqrt{4(\eta + v^2) - \beta^2}} \right\}.$$

In the absence of dispersion this reduces to $-\pi\omega_s/2v$.

For large distances to the surface the small momentum behavior dominates in the potential. Introducing dispersion in σ_Q^2 through the term $\beta\omega_s Q$ the image potential is found to be from Eq. (6.1),

$$\phi^I(z) = \frac{-1}{4z} + \frac{\beta}{8\omega_s}\frac{1}{z^2} - \frac{v\Theta(v)}{\omega_s}\left\{\frac{[1-(\beta/2v)^2]\sin(\omega_s z/v)+(\beta/v)\cos(\omega_s z/v)}{[1+(\beta/2v)^2]^2}\right\}\frac{1}{z^2} + O\left[\frac{1}{z^3}\right].$$

For an IN trajectory the correction with respect to the classical result is independent of the velocity as in the parallel case. In the SRM with the HA dielectric function, the image potential becomes

$$\phi^I(z) = \frac{-1}{4z} + \frac{\beta}{4\omega_p}\frac{1}{z^2} - \frac{v\Theta(v)}{\omega_s}\left\{\frac{[1-(3\beta/4v)^2]\sin(\omega_s z/v)+[\frac{3}{2}-(\beta/4v)^2](\beta/v)\cos(\omega_s z/v)}{[1+\beta^2/v^2][1+(\beta/4v)^2]^2}\right\}\frac{1}{z^2} + O\left[\frac{1}{z^3}\right],$$
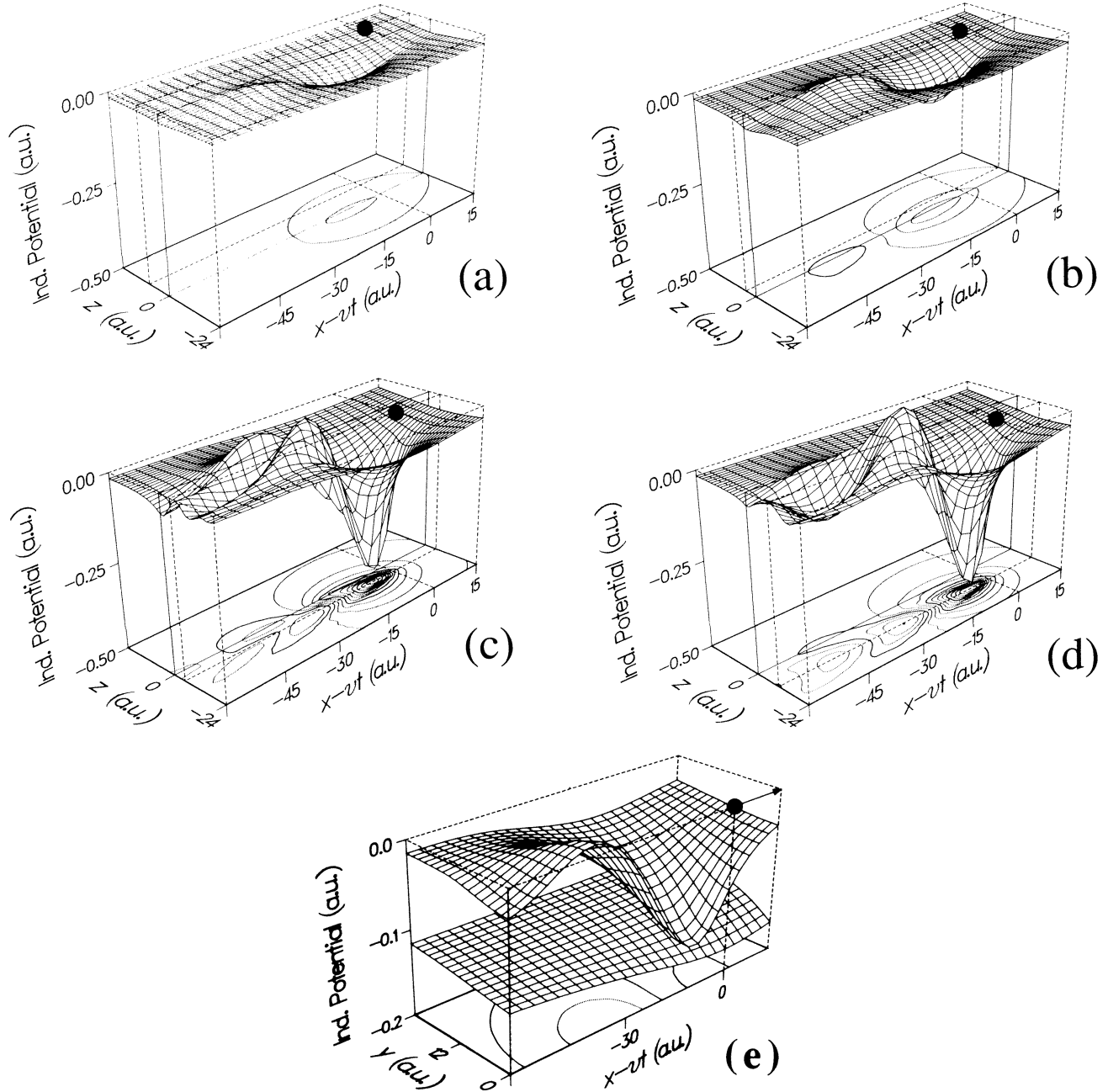

FIG. 2. Induced surface wake potential created by a proton, which is moving near an Al-vacuum interface ($r_s = 2$, $\gamma = 0.2$ a.u.) with velocity $v = 4$ a.u. from left to right. The proton has been represented by a black circle. The surface is described by the SRM with the PLA dielectric function. The wake potential is shown in the plane perpendicular to the surface and containing the trajectory for four different separations of the proton with respect to the surface: (a) $z_0 = 10$ a.u.; (b) $z_0 = 5$ a.u.; (c) $z_0 = -5$ a.u.; (d) $z_0 = -10$ a.u. It is also plotted in a plane parallel with the surface for $z_0 = 5$ a.u. (e), $z = 0$ a.u. (upper sheet) and $z = 5$ (lower sheet; the potential has been shifted 0.1 a.u. downwards in this case). The solid is in the region $z < 0$. The distance between contour lines is 0.04 a.u.
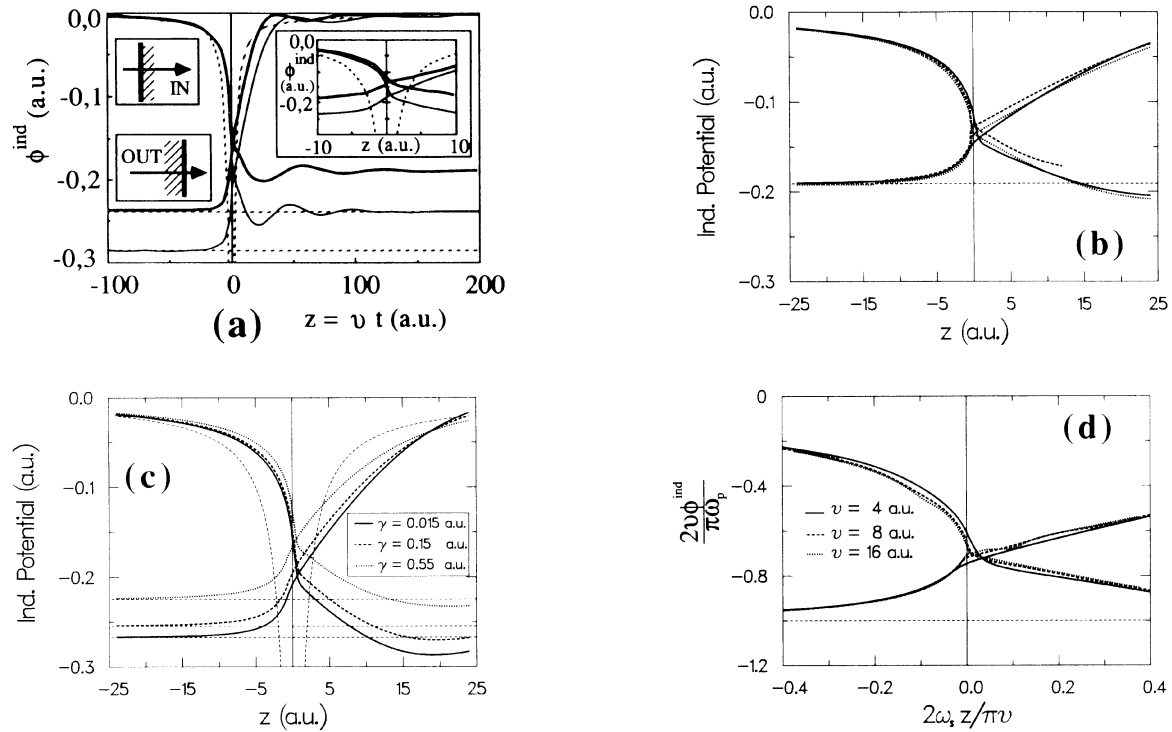
FIG. 3. Induced potential at the position of a proton traveling in the perpendicular direction to a solid-vacuum surface from left to right. (a) The velocities of the proton considered here are $v=5$ a.u. (solid curve) and $v=4$ a.u. (narrow curve) in both the OUT (solid at the left) and IN (solid at the right) cases. We have taken $r_s=2$ and $\gamma=0.015$ a.u. The SRM has been used with the PLA dielectric function, Eq. (3.14), to describe the bulk solid. The bulk limit and the classical induced potential in the vacuum, $-1/2|z|$, are also included in the picture (broken lines). (b) Under the same conditions, with $v=5$ a.u., the results obtained from the local response approximation of Sec. II (dotted line), the Hamiltonian formulation (dashed line), and in the SRM with the PLA dielectric function (solid line) are compared here. (c) Effect of damping for $r_s=1.6$, $v=5$ a.u., and damping $\gamma=0.015, 0.15$, and 0.55 a.u. using the SRM and the PLA dielectric function. (d) Effect of the velocity for $r_s=3$, $\gamma=0.15$ a.u., and $v=4, 8$, and 16 a.u. using the SRM with the PLA dielectric function.

and this expression has a similar qualitative behavior as the previous one. In both cases the velocity-independent correction coincides with the full correction to order $1/z^2$ in the parallel case, and differs in a factor $\sqrt{2}$ from a model to the other. The interpretation given for this

term in the parallel case is valid here as well. The velocity-dependent term, present in the outgoing case, oscillates with frequency ω_s.

Figure 3(a) shows the induced potential at the position of the particle for the incoming (IN) and outgoing (OUT)
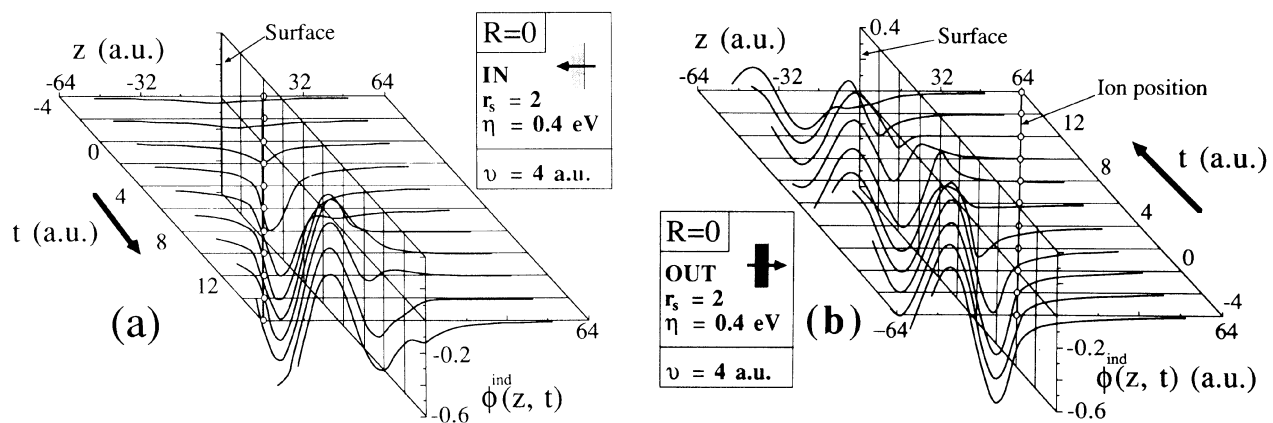

FIG. 4. Wake formation (a) and destruction (b) processes when a proton crosses a solid-vacuum interface following a perpendicular trajectory. The induced potential is plotted for points along the trajectory. The different positions of the ion for different times are represented by a chain of open circles in the zt plane. The parameters used in the calculation are shown in the figure.

trajectories calculated in the SRM with the PLA dielectric function to describe the bulk solid. Before the particle has crossed the surface, the potential deviates itself very much from the classical induced potential in the vacuum and from the bulk value in the solid only in the region $|z| < \pi v / 2\omega_p$. The oscillations that appear once the particle has crossed the surface correspond to the frequency ω_s in the vacuum and to a superposition of frequencies ω_s and ω_p in the solid. The wavelength of those oscillations increases with v [see Fig. 3(a)]. In Fig. 3(b)
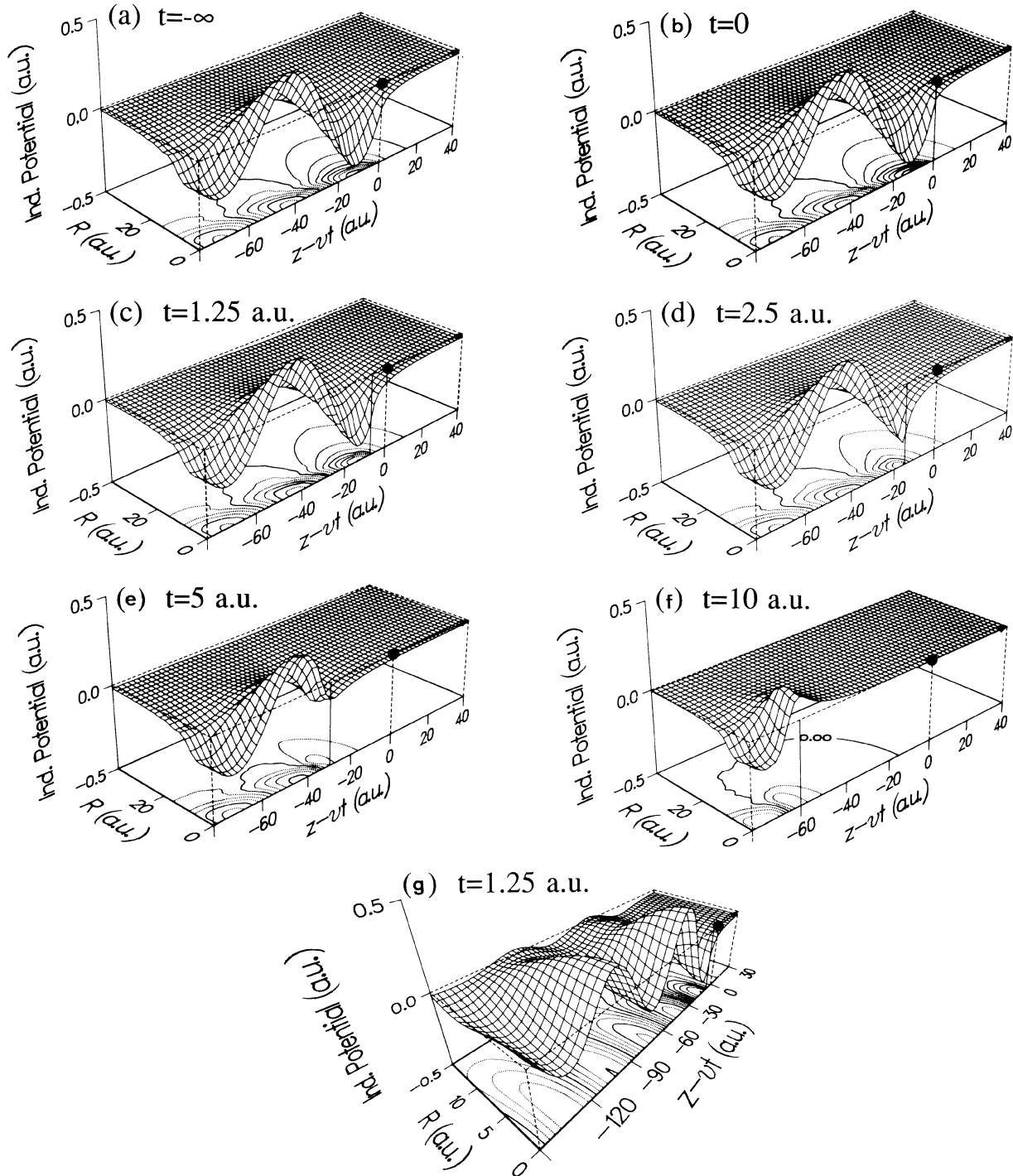

FIG. 5. (a)–(f) Induced surface wake potential created by an outgoing proton that crosses an Al-vacuum surface ($r_s = 2$, $\gamma = 0.015$ a.u.) in a perpendicular direction to the surface. The solid is in the region $z < 0$. The SRM and PLA have been used. The particle velocity is $v = 6$ a.u. The proton, plotted here as a black circle, reaches the surface at $t = 0$. The wake is plotted on a grid in $z - vt$ and R for different times as shown in the figure. For finite times the surface is represented by a vertical solid line. The contour line increment is 0.05 a.u. (g) The same as (a)–(f) for $t = 1.25$ and for a different region in the plane (R, z), which allows us to see the Mach-cone structure in the surface wake.

the SRM results are compared with the ones obtained from Eqs. (4.1), (4.3), and (6.1) in the Hamiltonian formulation: Before the particle has crossed the surface both models give quite similar results except near the surface ($|z| < \pi v/10\omega_s$). In fact, the Hamiltonian formulation gives the same value for the induced potential at the surface ($z = 0$) in the IN and OUT trajectories and that is not the case in the SRM: The magnitude of the induced potential at the surface is smaller in the IN trajectory. After the particle has crossed the surface the results differ significantly in the region $|z| < \pi v/2\omega_p$. In Figs. 3(c) and 3(d) we show the influence of damping and velocity on the induced potential. The conclusions that can be drawn are the same as in the parallel case: The smaller the damping or the velocity the closer to the surface are the bulk limit and the classical induced potential in the vacuum reached. For an OUT particle moving in the vacuum side the surface-plasma-induced oscillations seem to be attenuated with the damping [see Fig. 3(c) in the upper right corner]. The difference $\phi_{IN}^{ind}(z=0) - \phi_{OUT}^{ind}(z=0)$ goes to 0 like $1/v^2$ in the large-velocity limit[10,12] [see Fig. 3(d)].

The evolution of the surface wake potential is shown in Fig. 4 for points along the trajectory in the IN and OUT cases and in Fig. 5 for points not exclusively in the trajectory but only in the OUT case. The SRM, using the PLA, has been adopted. The bulk wake is seen to remain almost unchanged until the particle has crossed the surface in the OUT case and even when the ion is in the vacuum the potential in the solid resembles very much the bulk wake. This picture is not valid for points near the surface ($|z| < \pi v/2\omega_p$). It indicates that

$$\phi^{ind}(\mathbf{r},t) = \phi^{\infty}(\mathbf{r} - \mathbf{v}t, \mathbf{v})\Theta(-z)$$

may constitute a good approximation to the surface wake potential. The first minimum of the potential, as it appears in the bulk wake, is formed after a time $\approx \pi/\omega_p$ once the charge has crossed the surface in the IN case [see Fig. 4(a)].

VII. SUMMARY

The surface wake potential created by a swift charged point particle moving close to a planar solid-vacuum interface has been analyzed from two different points of view: the well-known Hamiltonian formulation based on the plasma modes, and the specular-reflection model using different nonlocal approximations to the bulk dielectric function. The latter has been used to picture the surface wake in the cases of parallel and perpendicular motion.

Under parallel motion conditions, when the ion follows an external trajectory, the surface wake presents a maximum and a minimum resembling the bulk wake, but their distance from the particle is $\sqrt{2}$ times larger. The surface wake is practically the bulk wake when the ion is traveling at a distance larger than $\pi v/2\omega_p$ from the surface inside the solid.

When the charge moves perpendicular to the surface and toward the vacuum, the potential in the solid side turns out to be the bulk wake potential until the particle has almost reached the surface. When the ion penetrates the solid the wake formation takes a time $\approx \pi/\omega_p$. The oscillations in the potential of frequency ω_s after the particle has crossed the surface are well reproduced in both models.

The influence of damping in the plasma modes on the induced potential has also been studied and the results are the same as in the bulk wake potential:[66] attenuation of the potential for increasing damping. This effect is stronger in the solid side.

ACKNOWLEDGMENTS

[1] R. H. Ritchie, Phys. Rev. **106**, 874 (1957).

[2] N. Takimoto, Phys. Rev. **146**, 366 (1966).

[3] N. G. van Kampen, B. R. A. Nijboer, and K. Schram, Phys. Lett. **26A**, 307 (1968); E. Gerlach, Phys. Rev. B **4**, 393 (1971).

[4] A. A. Lucas, Phys. Rev. B **4**, 2939 (1971).

[5] G. D. Mahan, Phys. Rev. B **5**, 739 (1972).

[6] P. J. Feibelman, Surf. Sci. **27**, 438 (1971); P. J. Feibelman, C. B. Duke, and A. Bagchi, Phys. Rev. B **5**, 2436 (1972).

[7] R. H. Ritchie, Phys. Lett. **38A**, 189 (1972).

[8] J. Harris and R. O. Jones, J. Phys. C **6**, 3585 (1973); **7**, 3751 (1974).

[9] J. Heinrichs, Phys. Rev. B **8**, 1346 (1973).

[10] D. Chan and P. Richmond, J. Phys. C **9**, 163 (1976).

[11] M. Šunjić, G. Toulouse, and A. A. Lucas, Solid State Commun. **11**, 1629 (1972).

[12] R. Ray and G. D. Mahan, Phys. Lett. **42A**, 301 (1972).

[13] D. Chan and P. Richmond, Surf. Sci. **39**, 437 (1973).

[14] F. Flores and F. García-Moliner, J. Phys. C **12**, 907 (1979).

[15] L. Hedin and S. Lundqvist, Solid State Phys. **23**, 1 (1969).

[16] P. M. Echenique, R. H. Ritchie, N. Barberán, and J. Inkson, Phys. Rev. B **23**, 6486 (1981).

[17] F. Sols and R. H. Ritchie, Surf. Sci. **194**, 275 (1988); Solid State Commun. **63**, 245 (1987); Phys. Rev. B **35**, 9314 (1987).

[18] J. R. Manson and R. H. Ritchie, Phys. Rev. B **24**, 4867 (1981); for a review and applications of the formalism, see J. R. Manson, R. H. Ritchie, P. M. Echenique, A. Gras-Martí, and T. L. Ferrell, Phys. Scr. **39**, 725 (1989).

[19] X.-Y. Zheng, R. H. Ritchie, and J. R. Manson, Phys. Rev. B **39**, 13 510 (1989).

[20] H. G. Eriksson, B. R. Karlsson, and K. A. I. L. Wijewardena, Phys. Rev. B **31**, 843 (1985).

[21] R. H. Ritchie and A. L. Marusak, Surf. Sci. **4**, 234 (1966).

[22] D. Wagner, Z. Naturforsch. Teil A **21**, 634 (1966).

[23] J. Neufeld and R. H. Ritchie, Phys. Rev. **98**, 1632 (1955); **99**, 1125 (1955).

[24] V. N. Neelavathi, R. H. Ritchie, and W. Brandt, Phys. Rev.

Lett. **33**, 302 (1974); **33**, 670(E) (1974); **34**, 560(E) (1975); R. H. Ritchie, W. Brandt, and P. M. Echenique, Phys. Rev. B **14**, 4808 (1976); P. M. Echenique, R. H. Ritchie, and W. Brandt, *ibid.* **20**, 2567 (1979).

[25]R. H. Ritchie and P. M. Echenique, Philos. Mag. A **45**, 347 (1982); A. Mazarro, P. M. Echenique, and R. H. Ritchie, Phys. Rev. B **27**, 4117 (1983); P. M. Echenique, F. Flores, and R. H. Ritchie, Solid State Phys. **43**, 229 (1990).

[26]H. Rothard *et al.*, J. Phys. C **21**, 5033 (1988); for a review on convoy-electron experiments see M. Breinig *et al.*, Phys. Rev. A **25**, 3015 (1982).

[27]L. F. Ferrariis and R. A. Baragiola, Phys. Rev. A **33**, 4449 (1986); H. Winter, P. Strohmeier, and J. Burgdörfer, *ibid.* **39**, 3895 (1989); M. Hasegawa, T. Uchida, K. Kimura, and M. Mannami, Phys. Lett. A **145**, 182 (1990).

[28]M. Burkhard *et al.*, Phys. Rev. Lett. **58**, 1773 (1987); H. Rothard *et al.*, J. Phys. (Paris) Colloq. **50**, C2-105 (1989).

[29]See, for instance, K. O. Groeneveld, R. Maier, and H. Rothard, Nuovo Cimento **12**, 843 (1990), and the references therein.

[30]Y. Yamazaki, Proceedings of the NATO Advanced Study Institute, Aliconte (1990), edited by A. Gras-Martí *et al.* (Plenum, New York, 1991), p. 423; Y. Yamazaki, K. Kurobi, F. Fujimoto, L. H. Andersen, P. Hvelplund, H. Knudsen, S. P. Møller, E. Uggerhøj, and K. Elsener (unpublished); Y. Yamazaki, Nucl. Instrum. Methods B **48**, 97 (1990).

[31]P. M. Echenique and R. H. Ritchie, Phys. Lett. **111A**, 310 (1985); A. Rivacoba and P. M. Echenique, Phys. Rev. B **36**, 2277 (1987); J. Burgdörfer, J. Wang, and J. Müller, Phys. Rev. Lett. **62**, 1599 (1989); F. J. García de Abajo, P. M. Echenique, and R. H. Ritchie, Nucl. Instrum. Methods B **48**, 25 (1990).

[32]T. Iitaka, Y. H. Ohtsuki, A. Koyama, and H. Ishikawa, Phys. Rev. Lett. **65**, 3160 (1990).

[33]A. Koyama, Y. Sasa, H. Ishikawa, A. Misu, K. Ishii, T. Iitaka, Y. H. Ohtsuki, and M. Uda, Phys. Rev. Lett. **65**, 3156 (1990).

[34]K. Kimura, M. Hasegawa, Y. Fujii, M. Suzuki, Y. Susuki, and M. Mannami, Nucl. Instrum. Methods B **33**, 358 (1988).

[35]Y. H. Ohtsuki, T. O'hori, and R. Kawai, Nucl. Instrum. Methods **194**, 35 (1982); T. O'hori and Y. H. Ohtsuki, Phys. Rev. B **27**, 3418 (1983).

[36]Y. Susuki, H. Mukai, K. Kimura, and M. Mannami, Nucl. Instrum. Methods B **48**, 347 (1990); H. Winter, J. C. Poizat, and J. Remillieux (unpublished); H. Winter (unpublished).

[37]R. G. Barrera and C. B. Duke, Phys. Rev. B **13**, 4477 (1976).

[38]P. M. Echenique, Ph.D. thesis, Universidad Autónoma de Barcelona, 1977 (unpublished).

[39]P. M. Echenique and J. B. Pendry, J. Phys. C **8**, 2936 (1975); J. P. Muscat and D. M. Newns, Surf. Sci. **64**, 641 (1977); Yu. A. Romanov and V. Ya. Aleshkin, Fiz. Tverd. Tela (Leningrad) **23**, 86 (1981) [Sov. Phys. Solid State **23**, 47 (1981)].

[40]N. Barberán, P. M. Echenique, and J. Viñas, J. Phys. C **12**, L111 (1979).

[41]K. Suzuki, M. Kitagawa, and Y. H. Ohtsuki, Phys. Status

Solidi B **82**, 643 (1977); Y. H. Ohtsuki, *Charged Beam Interaction With Solids* (Taylor & Francis, London, 1983).

[42]F. García-Moliner and F. Flores, *Introduction to the Theory of Solid Surfaces* (Cambridge University Press, Cambridge, England, 1979).

[43]R. Núñez, P. M. Echenique, and R. H. Ritchie, J. Phys. C **13**, 4229 (1980); P. M. Echenique, Philos. Mag. B **52**, L9 (1985); N. Zabala and P. M. Echenique, Ultramicroscopy **32**, 327 (1990); A. Gras-Martí, P. M. Echenique, and R. H. Ritchie, Surf. Sci. **173**, 310 (1986).

[44]G. Gumbs and M. L. Glasser, Phys. Rev. B **37**, 1391 (1988).

[45]D. M. Newns, Phys. Rev. B **1**, 3304 (1970).

[46]Z. Penzar and M. Šunjuć, Phys. Scr. **30**, 453 (1984).

[47]F. Bloch, Z. Phys. **81**, 363 (1933); Helv. Phys. Acta **7**, 385 (1934).

[48]B. I. Lundqvist, Phys. Kondens. Mater. **6**, 206 (1967); Phys. Status Solidi **32**, 273 (1969).

[49]A. W. Overhauser, Phys. Rev. B **3**, 1888 (1971).

[50]J. I. Gersten and N. Tzoar, Phys. Rev. B **8**, 5671 (1973).

[51]A. A. Lucas, E. Kartheuser, and R. C. Badro, Phys. Rev. B **2**, 2488 (1970).

[52]A. A. Lucas and M. Šunjić, Phys. Rev. Lett. **26**, 229 (1971); M. Šunjić and A. A. Lucas, Phys. Rev. B **3**, 719 (1971); A. A. Lucas and M. Šunjić, Prog. Surf. Sci. **2**, 75 (1972).

[53]G. D. Mahan, *Collective Properties of Physical Systems*, Nobel Symposium No. 24 (Academic, New York, 1973), p. 164.

[54]B. Gumhalter and D. M. Newns, Surf. Sci. **50**, 465 (1975).

[55]A. G. Eguiluz, Solid State Commun. **33**, 21 (1980).

[56]J. W. Wu and G. D. Mahan, Phys. Rev. B **28**, 4839 (1983).

[57]J. Mahanty, K. N. Pathak, and V. V. Paranjape, Solid State Commun. **54**, 649 (1985); Phys. Rev. B **33**, 2333 (1986).

[58]R. Kawai, N. Itoh, and Y. H. Ohtsuki, Surf. Sci. **114**, 137 (1982).

[59]T. Iitaka and Y. H. Ohtsuki, Surf. Sci. **213**, 187 (1989).

[60]A. Galindo and P. Pascual, *Mecánica Cuántica* (Editorial Alhambra, Madrid, Spain, 1978).

[61]B. N. Libenson and V. V. Rumyantsev, Zh. Eksp. Teor. Fiz. **86**, 1715 (1984) [Sov. Phys. JETP **59**, 999 (1984)]; J. P. Muscat, Solid State Commun. **18**, 1089 (1976).

[62]N. J. M. Horing, H. C. Tso, and G. Gumbs, Phys. Rev. B **36**, 1588 (1987).

[63]Y. H. Ohtsuki, K. Koyama, and Y. Yamamura, Phys. Rev. B **20**, 5044 (1979); Y. H. Ohtsuki, R. Kawai, and K. Tange, Nucl. Instrum. Methods B **13**, 193 (1986); K. J. Snowdon, D. J. O'Connor, and R. J. MacDonald, Phys. Rev. Lett. **61**, 1760 (1988); M. Kato, T. Iitaka, and Y. H. Ohtsuki, Nucl. Instrum. Methods B **33**, 432 (1988); Y. Ono, T. Miyamoto, T. Iitaka, and Y. H. Ohtsuki, Radiat. Eff. Express **2**, 63 (1988).

[64]J. A. Appelbaum and D. R. Hamann, Phys. Rev. B **6**, 1122 (1972).

[65]N. D. Lang and W. Kohn, Phys. Rev. B **7**, 3541 (1973); B. N. J. Persson and P. Apell, *ibid.* **27**, 6058 (1983).

[66]J. C. Ashley and P. M. Echenique, Phys. Rev. B **31**, 4655 (1985).